TRANSPORT PROBLEMS 2023 Volume 18 Issue 3
PROBLEMY TRANSPORTU DOI: 10.20858/tp.2023.18.3.16

Keywords: hydrogen engine; 3D mathematical modeling; annular gap; flame propagation

Revaz KAVTARADZE[1]*, Tamaz NATRIASHVILI[2], Merab GLONTI[3], Giorgi CHILASVILI[4], Otar GELASHVILI[5], Jumber IOSEBIDZE[6]

FLAME PROPAGATION IN A NARROW GAP BETWEEN THE PISTON AND CYLINDER OF A HYDROGEN ENGINE

Summary. The processes of flame penetration and propagation in a narrow annular gap between the piston and cylinder of a hydrogen piston engine are investigated by the method of 3D mathematical modeling. The model is verified by comparing the changes in pressure and heat release rate in the cylinder obtained from an experimental hydrogen engine, considering the data collected during numerical experiments. The movement of the flame front into the gap is analyzed by changes in the instantaneous local values of the hydrogen fractions in the mixture and the local temperatures of the cold gas (unburned mixture) and combustion products. A comparative analysis of the spread of gasoline and hydrogen flames is carried out. The phenomenon of increasing heat losses in the combustion chamber of a hydrogen engine compared to a gasoline engine, previously confirmed experimentally by different authors and not yet having an acceptable theoretical interpretation, is explained by neglecting the role of heat transfer in the indicated gap.

1. INTRODUCTION

Experimental studies were carried out on a serial gasoline engine CA20 for a passenger car converted to hydrogen with the injection of hydrogen gas into the intake system. At the same time, in the hydrogen version of the engine, two hydrogen injectors were installed in front of each cylinder in the intake system to provide the necessary cycle dose of hydrogen. The main technical data of the engine are given in Table 1.

Fig. 1a schematically shows the diametral section of the 3D cylinder structure, and Fig. 1b shows the piston with the indication of the fiery belt surface, which is a part of the inner surface of the annular gap between the piston and the cylinder, located above the upper compression ring (further for brevity, see "gap"). With the movement of the piston, the gap moves along the surface of the cylinder (i.e., another

[1] Rafael Dvali Institute of Machine Mechanics; 10 Mindeli Str., Tbilisi 0186, Georgia; e-mail: rzkavtaradze@gmail.com; orcid.org/0000-0001-9585-9245
[2] Rafael Dvali Institute of Machine Mechanics; 10 Mindeli Str., Tbilisi 0186, Georgia; e-mail: t_natriashvili@yahoo.com; orcid.org/0000-0001-9141-3641
[3] Rafael Dvali Institute of Machine Mechanics; 10 Mindeli Str., Tbilisi 0186, Georgia; e-mail: merabglonti@gmail.com; orcid.org/0000-0003-2711-5089
[4] Rafael Dvali Institute of Machine Mechanics; 10 Mindeli Str., Tbilisi 0186, Georgia; e-mail: chilashvili.gia@gmail.com; orcid.org/0009-0006-4902-9076
[5] Georgian Technical University; 77 Merab Kostava Str., Tbilisi 0171, Georgia; e-mail: gelashviliotar@gtu.ge; orcid.org/0009-0002-4055-1176
[6] Georgian Technical University; 77 Merab Kostava Str., Tbilisi 0171, Georgia; e-mail: j.iosebidze@gtu.ge; orcid.org/0009-0009-2591-9973
* Corresponding author. E-mail: rzkavtaradze@gmail.com

part of its inner surface relating to the engine cylinder) changes, while its volume remains constant. We emphasize that the belt can be called a fiery surface only if the flame penetrates into the gap.

The processes of the movement of the combustible mixture, combustion, propagation of the flame front, as well as the formation of nitrogen oxides and heat exchange with the walls are modeled both in the volume of the combustion chamber and in the volume of the annular gap.

Table 1

Main technical data of the engine

Parameters/dimensions	Value
Number of cylinders	4
Cylinder diameter/piston stroke, D/S, mm/mm	86/86
Compression ratio, ε, -	10
Cooling	Liquid
Power, N_e, kW	60 (at n=5500 min^{-1})
Torque, M_{max}, Nm	111 (at n=4000 min^{-1})

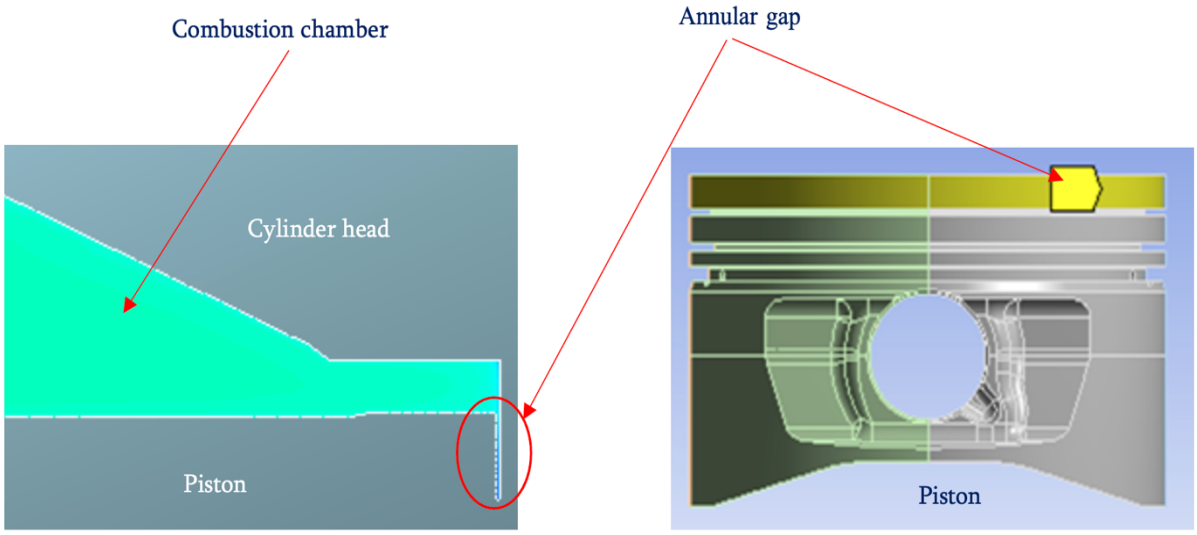

a) b)

Fig. 1. a) the combustion chamber and the annular gap between the piston and the cylinder above the upper piston ring (axial section) and b) the piston fiery belt with a width of 5.5 mm

The applied mathematical model is based on the fundamental equations of momentum (Navier-Stokes equations), energy (Fourier-Kirchhoff equation), diffusion (Fick equation), and continuity equation. After averaging by the Favre method, RANS models of turbulence are added to these equations (in particular, the k-ζ-f Hanjalich model), as well as burning models (coherent flame model), the formation of nitrogen oxides NO_x (the thermal mechanism of Zeldovich), and the model of heat exchange in the boundary layer (Wall functions of Spalding–Patankar [1]). The description of these models and their features related to the specifics of processes in piston engines, as well as the procedures of the numerical solution by the control volume method, are described in [2, 3].

In this study, the minimum size of the control volume (calculated cell) was 0.07 mm, and numerical experiments were carried out for two variants of the annular gap. The total number of calculated cells with a gap l_h = 0.2 mm at the time the piston is at the top dead center is 606,453 in the volume of the combustion chamber; in the volume of the gap itself, this number is almost 150,000. In the case of a gap with a size of l_h = 0.35 mm, these numbers of control volumes are 642,902 and 185,000, respectively. A

3D mathematical model of thermophysical processes occurring in both the combustion chamber and the gap is implemented using the AVL FIRE CRFD program [1].

2. 3D MODELING OF PROCESSES IN THE COMBUSTION CHAMBER: VERIFICATION OF THE MODEL

Unsteady processes of turbulent motion of the working fluid, combustion, flame propagation, heat release, heat exchange between the working fluid, the walls of the combustion chamber, and formation of nitrogen oxides in the combustion chamber were simulated. The simulation was carried out for all typical operating modes of the experimental hydrogen engine. The load conditions were modeled for different values of the excess air coefficient (a_{air}=1.0, 1.64, 2.0, and ∞), with $\alpha_{air}=\infty$ meaning that only air enters the cylinder and no fuel is supplied. Then, this cylinder works in compressor mode of compression-expansion, or, in other words, in scroll mode. It should be emphasized that experimental studies were conducted on lean hydrogen-air mixtures ($\alpha_{air}>1.6$) in order to prevent abnormal processes of hydrogen combustion (detonation, backfire, premature ignition, or surface ignition). The 3D model of the working process was verified by comparing the experimental and calculated indicator diagrams, averaged by the volume of combustion chamber temperatures of the working fluid and heat release rates obtained on their basis. Figs. 2 and 3, which show examples of verification, indicate a good agreement between experimental and calculated data. Note that in these and subsequent figures, the designation φ is the angle of rotation of the crankshaft (CA).

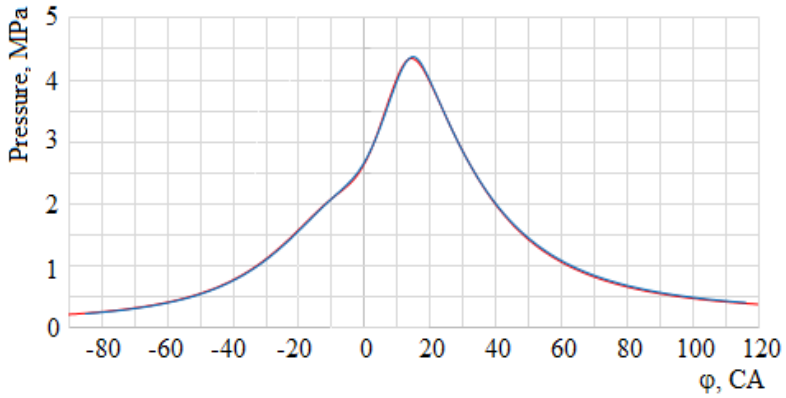

Fig. 2. Comparison of the unsteady pressures in the combustion chamber of a hydrogen engine, obtained by simulation and experimental studies, with n=3000 min^{-1} and α_{air}=1,64. Experimental data are shown in red; calculated data are shown in blue

Following the recommendations of [1], the used 3D mathematical hydrogen engine workflow model was verified using the following values of the initial parameters and initialization parameters: specified value of the compression ratio ε≈9.8, initial calculation angle φ_{in}=633° (-87° from TDC), initial pressure p_{in}=212 996 Pa, initial temperature T_{in}=500K, initial gas density ρ_{in}=1.43 kg/m^3, initial kinetic energy of turbulence k_{in}=25.4 m^2/s^2, initial turbulence linear scale l_t= 0.00171833 m, parameter for initializing the vortex motion SW=300 min^{-1}, parameter for initializing the stretching of the flame front SF=6.1, and parameter for initializing the initial density of the flame surface IFSD=2500 m^{-1}.

The 3D workflow model used includes a coherent flame model [1], in which the flame development is described by the surface density of the flame, which is the surface area of the flame per unit volume. The IFSD parameter is a constant of the combustion model and is intended for its control. Its value is required for calculated cells (control volumes) of the grid in which ignition occurs. It affects the ignition delay: the higher the initial value of the flame density, the shorter the ignition delay. The SF parameter is also a constant of the combustion model and is used to control the duration of the combustion phase. Its increase leads to an intensification of the formation of the surface density of the flame and, consequently, to a shorter (fast-flowing) combustion phase.

In the beginning, the velocity field in the cylinder is initialized by the vortex flow, the intensity of movement of which is determined based on the vortex number (Ricardo number) measured during the bench tests depending on the rotational speed of the crankshaft. In the absence of such possibilities, its approximate value is selected according to known data and specified by trial calculations.

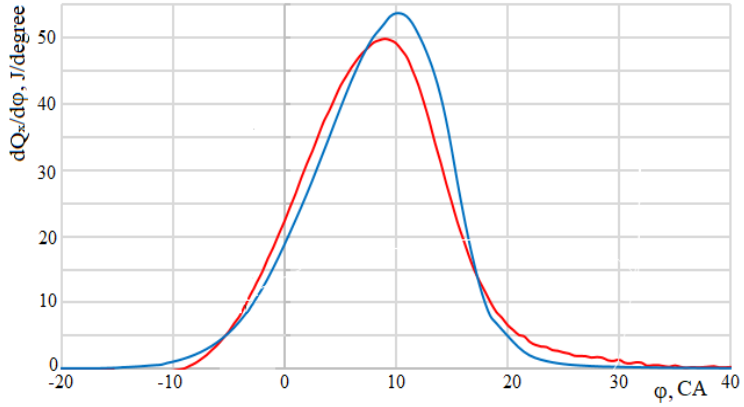

Fig. 3. Comparison of the heat release rates in the combustion chamber of a hydrogen engine obtained by modeling and measuring the pressure (Fig. 2) in the mode n=3000 min-1 and αair=1.64. Experimental data are indicated in red; calculated data are indicated in blue

We emphasize that the above parameter values lead to a good agreement between the calculated and experimental pressure diagrams (Fig. 2) and the heat release rate (Fig. 3). The results of modeling the emission of nitrogen oxides ([NOx] = 2440 ppm) for this mode are also in good agreement with the results of direct measurement ([NOx] = 2242 ppm (difference Δ= 8.8 %. Similar to the example given, the mathematical model of the working process of a hydrogen engine with spark ignition was verified in all the studied modes of its operation.

Fig. 4 shows the results of the modeling and experimental investigation of the effect of the ignition advance angle on the emission of nitrogen oxides at the high-speed operation of a hydrogen engine n=3000 min^{-1}. The maximum deviation of the simulation results from the experimental data, as can be seen, is observed at the value of the CA φ_{ign}=15º and does not exceed 11%. The analysis of experimental indicator diagrams and the heat release rates dQx/dφ=f(φ) obtained on their basis indicates that at φ_{ign}=15º, compared with other values of φ_{ign}<15º, the highest values of the maximum cycle pressure p_z and the heat release rate $(dQx/d\varphi)_{max}$ are obtained. The locations of these peak values relative to the upper dead center on the graph p= (φ) at φ_{ign}=15º are the most favorable, which indicates the efficiency of the hydrogen engine operating cycle (indicator efficiency in this mode according to experimental data η_i= 40.8%). Obviously, this is the result of the intensification of the combustion process, which simultaneously leads to increases in p_z, the maximum cycle temperature (in this case, T_z=2375K), and local temperatures at the flame front. An increase in the temperature level of the cycle is accompanied by an increase in the emission of nitrogen oxides. This explains the increase in [NO_x] with the increase in the ignition-timing angle (Fig. 4).

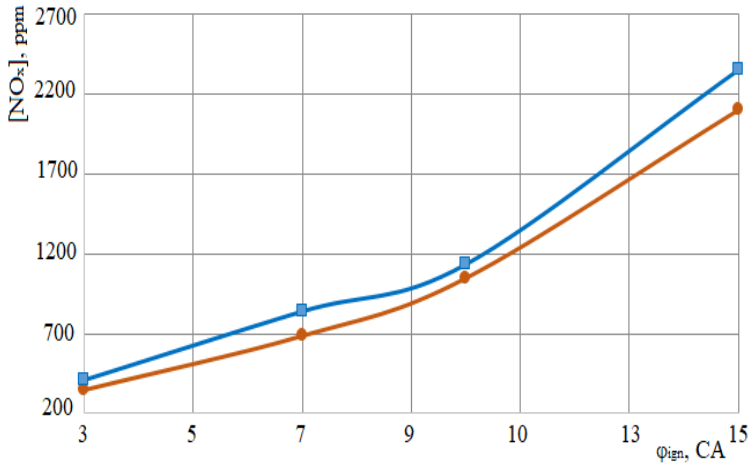

Fig. 4. The effect of the ignition advance angle on nitrogen oxide emissions (positive values φ_{ign} mean before the top dead center): a comparison of experimental (red) and calculated (blue) data. Mode n=3000 min^{-1}

3. THE CONDITION OF EXTINGUISHING THE FLAME IN THE COMBUSTION CHAMBER AND IN THE GAP

The flame spread in the combustion chamber is extinguished when approaching the cold walls and entering the gap (Fig. 1). According to the theory of Zeldovich [4,5], the flame goes out when the ratio of heat released in the flame to the heat diverted from the flame to the walls reaches a certain value, which is expressed by the number of Peclet, calculated as follows:

$$Pe_{1,2} = \frac{\rho \cdot c_p \cdot u_n}{\lambda} l_{1,2} = const, \quad (1)$$

where ρ, c_p, λ are the density, heat capacity at p=const, and thermal conductivity of the combustible mixture, respectively; u_n is the normal velocity of the flame front (velocity in the direction of the flame front normal); indices 1 and 2 indicate both cases (the wall and gap) of the flame extinguishing; and l_1 and l_2 are the critical dimensions (or flame extinguishing distances, FED) of the distance to the wall and the linear size of the gap, respectively. For example, for a pipe, the critical diameter is the minimum diameter through which the flame still penetrates into the pipe. Note that the value of the critical size (FED) depends on the type of fuel, pressure, the temperature and composition of the mixture, and the speed of the flame propagation.

According to the results of experimental observations, the critical values of the *Pe* number led to the extinguishing of the flame of a stoichiometric mixture of gasoline with air in the following conditions of the combustion chamber of a piston engine: Pe_1=8 on the wall and Pe_2=40 in the gaps [5]. In this case, l_1/ l_2=0.2, and the critical dimensions are of the following order:

$$\begin{gathered} 0.02 \text{ mm} < l_1 < 0.2 \text{ mm}; \\ 0.1 \text{ mm} < l_2 < 1.0 \text{ mm}. \end{gathered} \quad (2)$$

It was shown in [6] that the flame extinguishing condition for a gasoline engine converted to hydrogen has the following form:

$$l_{cr\ Gasoline} > l_h > l_{cr\ Hydrogen}, \quad (3)$$

where l_h=0.2 mm is the value of the annular gap between the piston and the cylinder above the upper ring for a hot engine operating in the mode of maximum load (on a stoichiometric mixture of gasoline and air). It is determined after heating the cylinder-piston group on the stand simulating the heat-stressed state of the engine parts.

The critical dimensions of the annular gap for gasoline $l_{cr\ Gasoline}$=0.5 mm and hydrogen $l_{cr\ Hydrogen}$=0.125 mm flame in this work, as in [7], are set on the basis of the following experimentally proven facts:

1. $l_{cr\,Hydrogen} < l_{cr\,Gasoline}$ [5].
2. In the case of parallel walls, l_{cr} is 65% of the d_{cr} of a cylindrical pipe [7].
3. For various fuel-air mixtures, the values of l_{cr} are usually obtained under atmospheric conditions [7]. In the combustion chamber, where the pressure p and temperature T are significantly higher compared to atmospheric parameters, , l_{cr} is significantly lower; this is confirmed by the extrapolation of the dependencies $l_{cr} \sim p^{-x}$ given in [7].
4. The value of l_{cr} depends on the composition of the mixture. With a stoichiometric mixture, it tends to be minimized (i.e., when $\alpha_{air} \rightarrow 1$, $l_{cr} \rightarrow min$) [7].

Note that $l_{cr\,Gasoline}$ is set to 0.5 mm, and $l_{cr\,Hydrogen}$ is set to 0.125 mm, which is consistent with the conditions (2).

4. 3D MODELING OF PROCESSES IN THE GAP

The high pressure in the combustion chamber (Fig. 2) fills the gap volume with a combustible mixture of air and hydrogen before the combustion process begins. In this regard, the propagation (or quenching) of a non-stationary flame in the gap can be judged by the proportions of hydrogen in the working fluid – in the still unburned volume of the working fluid, the proportion of hydrogen is maximized for the given coefficient of excess air α_{air}, and in the already burned volume, the proportion of hydrogen is closer to 0. This is clearly seen in Table 2, which depicts that the change in the mass fraction of hydrogen $\bar{m}_{H2}(x, y, z, \tau)$, depending on the time τ (or on the angle of rotation of the crankshaft φ), makes it possible to judge the propagation of a hydrogen flame in the gap between the piston and cylinder.

It is clearly seen that at φ=728º (φ=720º corresponds to TDC), the hydrogen flame of the stoichiometric mixture enters the gap, spreads through its volume, and 50º after TDC—that is, at φ=770º, almost the entire amount of hydrogen in the gap burns out ($\bar{m}_{H2} \approx 0$), and the flame goes out. Thus, when α_{air}=1, the area of the inner surface of the gap simultaneously with the fiery bottom of the piston is a fiery surface with intensive heat exchange between the burning working fluid and the walls. It is obvious that when the flame penetrates the gap, heat losses in the wall increase.

It should be noted that the issues of heat transfer in the gap are considered in a publication by one of the authors of this article [6], in which, in addition to the simulation results, data are given for measuring the non-stationary heat flow in the gap, in particular on the surface of a moving piston, in the case when the flame does not penetrate into the gap. These measurements, carried out directly on a running engine, confirm that, in this case, the heat flows in the gap are an order of magnitude lower than in the combustion chamber. It is also shown that a significant increase in the heat flow to the piston's heat belt when the flame penetrates into the gap significantly increases the thermal tension of the piston [6].

In the case of a depleted mixture (α_{air}=1.64 and α_{air}=2), the flame cannot penetrate into the gap, and heat generation does not occur in its volume. This is confirmed by the simulation results showing that in the case of α_{air}=1.64 and α_{air}=2 at time φ=770º, the gap volume is filled with an unburned mixture in which the hydrogen fraction is equal to its maximum (initial) value ($\bar{m}_{H2} \approx max$). Obviously, in this case, the inner surface of the gap is no longer a surface of intense heat exchange, and heat losses are reduced compared to the case of α_{air}=1.

The extinguishing of the flame almost immediately upon entering the gap is explained by the following factors:

1. Heat generation is lower at α_{air}>1 than at α_{air}=1.
2. The mixtures that differ from stoichiometric ones are characterized by the excess of one of the reagents: either a fuel (α_{air}<1) or an oxidizer (α_{air}>1). The heat released as a result of the combustion reaction in such mixtures is consumed not only for heating the resulting combustion products but also for heating the excess masses of reagents not involved in the reaction. The combustion temperature decreases, and therefore, so does u_n.

3. The value of u_n depends on the properties of the combustible mixture—primarily, its thermal conductivity. Hydrogen, having a high thermal conductivity (λ=0.172 W/(m·K), has a higher u_n than other gases; for example, the thermal conductivity of methane is λ=0.0307 W/(m·K). In depleted mixtures (α_{air}>1), a decrease in the proportion of hydrogen leads to a decrease in u_n.

Thus, by the time the spark is ignited, a part of the mixture already fills the gap, and it is not captured by the flame front if the flame from the chamber does not penetrate it. This part flows into the chamber by the end of combustion (during the expansion stroke). By this point, the temperature in the combustion chamber is such that the additional oxidation of hydrogen to combustion products with the heat release is possible. Such a delayed heat release cannot increase the efficiency of the engine's working cycle, but it can improve the operating condition of the NOx neutralizer. The possibility of remaining in the cylinder as a residual gas and being oxidized in the subsequent combustion cycle, as happens in the case of hydrocarbon fuels, is practically excluded in the case of hydrogen due to its easy flammability.

Table 3 shows enlarged fragments of instantaneous temperature fields of the working fluid in the gap for the two different geometric dimensions of the gap (l_h= 0.2 mm and l_h=0.35 mm), with other conditions being identical. The local values of non-stationary temperatures can also be used to judge the propagation of the flame into the gap. It can be seen that the hydrogen flame spreads faster in the gap volume with a stoichiometric mixture, with an increase in the geometric size of the gap. In addition, it is noticeable that, in any case, the flame elongates faster than it expands, which is due to intensive cooling in the wall areas, both on the piston side and on the cylinder side. An increase in the gap from l_h= 0.2 mm to l_h=0.35 mm reduces the intensity of heat transfer from the gas on the gap surface (i.e., it reduces heat losses into the wall and contributes to an increase in the temperature of combustion products in the gap by about 250K) (see Table 3).

Table 2

Change in the mass fraction of hydrogen $\bar{m}_{H2}$ in the gap at l_h = 0.2 mm and α_{air}=var

α_{air}= 1; φ=728º	α_{air}= 1; φ=740º	α_{air}= 1; φ =750º
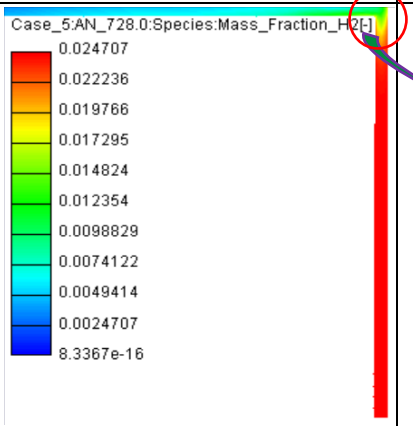	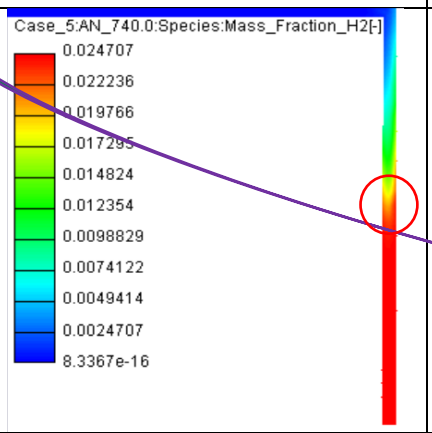	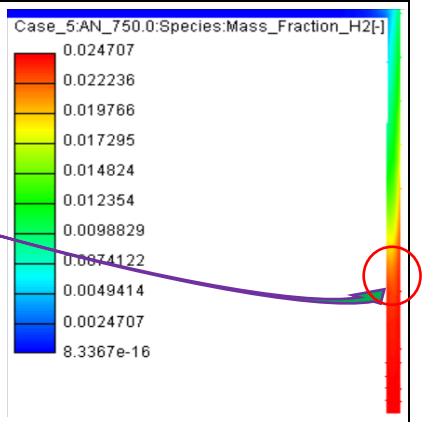
α_{air}= 1, φ=770º	α_{air}=1.64, φ=770º	α_{air}=2; φ=770º
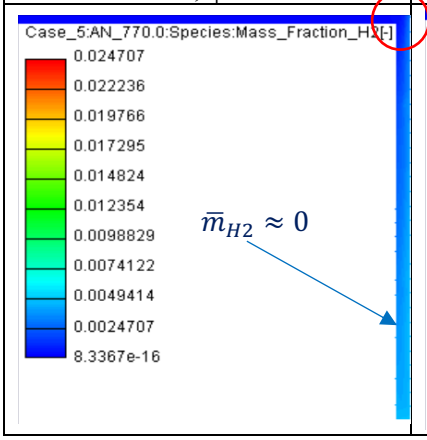	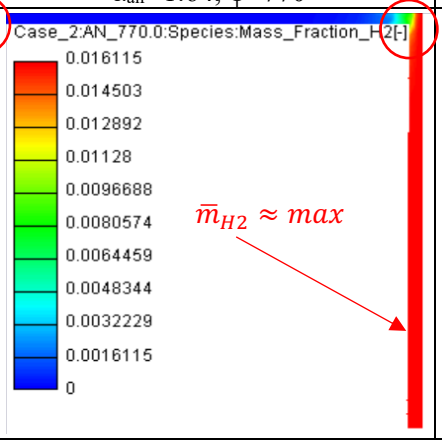	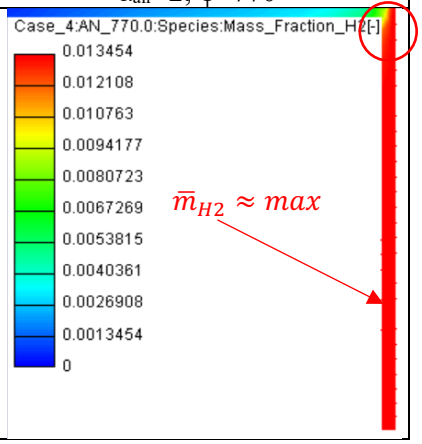

It should be noted that the local temperatures of the mixture in the gap in front of the flame front reach 900–1100 K (the part of Table 3 where the areas of such temperatures are circled), which is higher than the hydrogen self-ignition temperature (858 K). This indicates the possibility of the existence of the Mach effect in the gap. However, additional studies of thermophysical processes in the gap, including the velocity fields of the gas flow, are required to confirm this outcome.

5. CONCLUSIONS

The good agreement between the simulation results and experimental data—primarily regarding indicator diagrams, heat release rates, and nitrogen oxide emissions obtained by changing the ignition-timing angle—indicates the reliability of the verified model used in numerical experiments. The use of this model to study the environmental and effective characteristics of promising hydrogen engines with forced ignition can significantly reduce the time and cost of creating promising hydrogen engines and converting serial engines into hydrogen.

The process of hydrogen flame propagation into a narrow annular gap between the piston and the cylinder, located above the upper compression ring, is investigated for the first time in this study. The condition of hydrogen flame penetration is established, and it is shown that its propagation significantly depends on the composition of the combustible mixture.

Table 3

Enlarged fragments of instantaneous temperature fields of the working fluid in the gap for two different geometric dimensions of the gap (l_h=0.2 mm and l_h=0.35 mm) under identical conditions

α_{air}=1, n=3000 min^{-1}	α_{air}=1, n=3000 min^{-1}
ℓ_h=0.2 mm	ℓ_h=0.35 mm
T, K ↓ φ,^{0} → 730 740 750 760	T, K ↓ φ,^{0} → 730 740 750 760
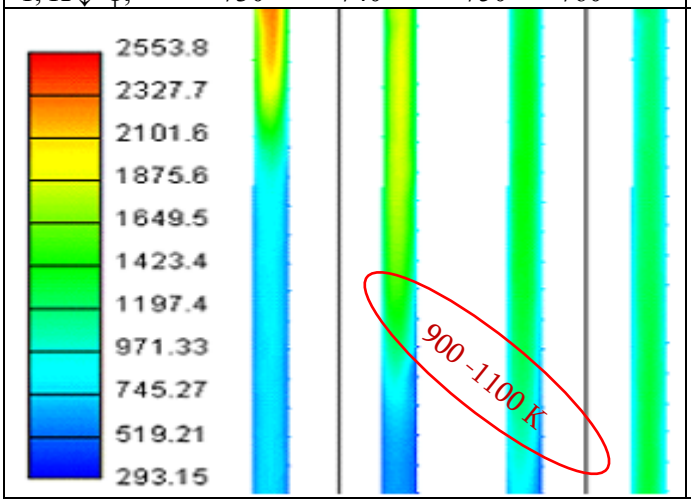	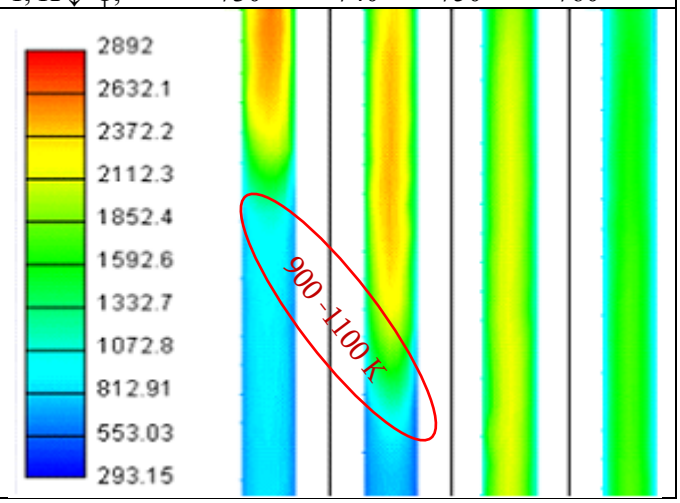

When a hydrogen flame penetrates into the gap, the combustion process in the gap clearly lags behind the combustion in the volume of the chamber (i.e., it is essentially the last phase of combustion: burning out in the cylinder).

Depending on the presence or absence of a flame in the gap, the thermal boundary conditions on the surface of the piston fiery belt change noticeably. Therefore, its heat-stressed state also changes. This is especially important to take into account when converting serial gasoline engines to hydrogen engines, in which the gasoline flame does not penetrate the gap, as shown in previous studies.

In the case of the hydrogen engine under study, the surface area of the piston fiery belt comprises 42% of the entire heat-absorbing surface of the piston over which the flame spreads. In the gasoline engine (the gap of which contains no flame), the surface is not a surface of active heat transfer from the

gas into the wall. In this regard, heat losses in the wall in a hydrogen engine will be significantly higher than in a gasoline engine. We emphasize that this phenomenon, which was experimentally confirmed earlier [8, 9], has not been given an acceptable theoretical explanation to date since it does not provide for the role of heat exchange in the specified gap. When working on a lean mixture, heat losses in the combustion chamber of a hydrogen engine decrease.

The propagation of the hydrogen flame through the gap volume with a stoichiometric mixture occurs faster as the geometric size of the gap increases.

References

1. *AVL FIRE. Users Manual*. AVL List GmbH, Graz, Austria. Version 2020.
2. Babayev, R. &, Andersson, A. & Dalmau, A.S. & Im Hong, G. & Johansson, B. Computational Characterization of Hydrogen Direct Injection and Nonpremixed Combustion in a Compression-Ignition Engine. *International Journal of Hydrogen Energy*. April 2021. 16 p.
3. Kavtaradze, R. & Natriashvili, T. & Gladyshev, S. Hydrogen-Diesel Engine: Problems and Prospects of Improving the Working Process. *SAE Society of Automotive Engineers (SAE), Technical Paper*. No. 2019-01-0541. USA, Detroit. 2019. 15 p.
4. Merker, G. & Schwarz, Ch. & Teichmann, R. (eds.) *Grundlagen Verbrennungsmotoren. Funktionsweise, Simulation, Messtechnik*. [In German: *Basics of internal combustion engines. Functionality, simulation, measurement technology*.]. Vieweg Teubner-Verlag. Springer Fachmedien, Wiesbaden GmbH. 2014. 795 p.
5. Merker, G. & Schwarz, Ch. & Stiesch, G. & Otto, F. *Verbrennungsmotoren. Simulation der Verbrennung und Schadstoffbildung*. [In German: *Internal combustion engines. Simulation of combustion and pollutant formation*]. Teubner-Verlag. Stuttgart, Leipzig, Wiesbaden, 2006. 410 p.
6. Kavtaradze, R.Z. & Onischenko, D.O. & Golosov, A.S. & Zelentsov, A.A. & Chen, Zh. & Sakhvadze, G.Zh. The Influence of the “Piston Heat Belt–Sleeve” Gap on Heat Exchange in the Combustion Chamber of an Engine Depending on the Fuel Utilized. *Journal of Machinery Manufacture and Reliability.* 2022. Vol. 51. No. 2. P. 112-120.
7. Onorati, A& Payri, R. & Vaglieco, B.M. & et al. The role of hydrogen for future internal combustion engines. *Int. Jour. Engine Research*. 2022. Vol. 23. No. 4. P. 529-540.
8. Shudo, T. Improving thermal efficiency by reducing cooling losses in hydrogen combustion engines. *International Journal of Hydrogen Energy*. 2007. No. 32. P. 4285-4293.
9. Demuynck, J. & De Paepe, M. & Verhaert, I. & Verhelst, S. Heat loss comparison between hydrogen, methane, gasoline and methanol in a spark-ignition internal combustion engine. *Energy Procedia*. 2012. Vol. 29. P. 138-146.

Received 21.01.2022; accepted in revised form 05.09.2023